Single phase DC/AC bi-directional converter with high-frequency isolation

Beristáin J. José A., Bordonau F. Josep, Busquets M. Sergi, Rocabert S. Joan and Murillo V. Ismael

***Abstract*— This paper introduces a comprehensive study of a dc/ac inverter with high-frequency isolation and bidirectional power flow capability. The topology is based on a high-frequency dc/ac converter, a high-frequency transformer, an ac/ac converter and a low-pass filter. In this scheme no additional dc-link stages are required. A LQR+I control approach and a modulation strategy for the commutation of the ac/ac converter switches is presented. Simulation and experimental verifications are provided.**

***Key words*— High Frequency Isolation, Bi-directional power flow, soft commutation and renewable energy.**

I. INTRODUCTION

Dc/ac inverter systems present a number of applications: induction motor drives, uninterruptible power supplies, photovoltaic energy systems, fuel cell systems, small wind power systems, etc. In many cases, isolation between the input and the output of the inverter is required, because of operating specifications or for security reasons. Significant contributions to conversion systems with HF (High Frequency) isolation can be found in [1]-[5]. The advantage of the idea studied in this paper is to have compact high-frequency isolation without any additional stage (usually a dc stage and a filter is required) and a simple control. The topology is divided in three parts: a high frequency dc/ac converter, a high-frequency transformer and an ac/ac converter.

A comprehensive study of the converter with galvanic isolation is presented in this work. The topology is used in [1],[4],[5]. A LQR+I control method that allows regulating the voltage and the output frequency is presented. The advantages of this structure are that it operates with output power up to 1 kW and has lower complexity (only two conversion stages are used, and without the need of dc-link filter). The LQR+I control provides an effective way to deal with multivariable controls typical in hybrid energy systems.

Manuscript received July 8, 2006. This work was supported by the Ministerio de Ciencia y Tecnología, Madrid, Spain, under Grant TIC-2002-03036, DPI 2000-0006-P4-02 and by ITSON-PROMEP, México..

Beristáin J. José A. is with the Instituto Tecnológico de Sonora, Electric and Electrónics Engineering Deparment; Av. Antonio Caso S/N Col. Villa ITSON; Ciudad Obregón, Sonora, México; C.P. 85138; Tel: (644) 4109000, ext. 1200; Fax: (644) 4109001.(e-mail bantonio@itson.,mx).

Bordonau F. Josep is with the Technical University of Catalonia, Electronic Engineering Department: Av. Diagonal 647, Despatx 9-24, Campus Sud - Edif. H, CP 08028 Barcelona, Sapain. (email josep.bordonau@upc.edu).

Busquets M. Sergi is with the Technical University of Catalonia, Electronic Engineering Department: DESPATX 212, Campus Terrasa- Edif. TR2C. Colom, CP 108222, Terrasa, Spain (email Sergio.busquets@upc.edu).

Rocabert S. Joan is with the Technical University of Catalonia, Electronic Engineering Department: Av. Diagonal 647, Despatx 9-24, Campus Sud - Edif. H, CP 08028 Barcelona, Sapain. (email rocabert@upc.edu).

Murillo V. Ismael is with the Instituto Tecnológico de Sonora, Electric and Electrónics Engineering Deparment; Av. Antonio Caso S/N Col. Villa ITSON; Ciudad Obregón, Sonora, México; C.P. 85138; Tel: (644) 4109000, ext. 1200; Fax: (644) 4109001.(e-mail imurillo@itson.,mx).

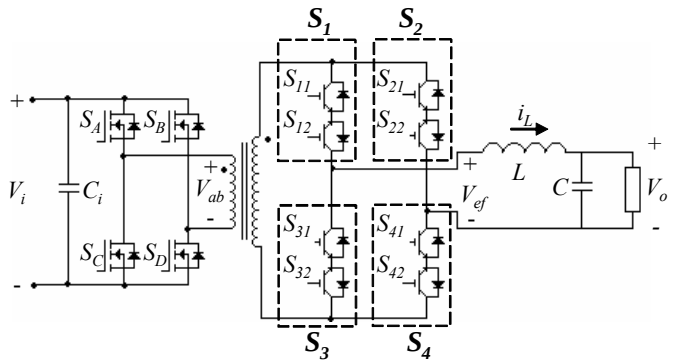

Fig. 1 DC/AC converter with high-frequency isolation.

II. DESCRIPTION AND CIRCUIT CONFIGURATION

The objective of the single-phase HF-Link inverter is to generate a sinusoidal voltage with galvanic isolation and bidirectional power flow capability. The topology used in this work is presented in Fig.1.

A. Inverter description

The single-phase inverter generates a high-frequency ac voltage at the transformer primary. It generates a high-frequency PWM voltage by means of closed-loop bipolar control. Bipolar voltage is needed because of the use of a HF transformer.

Fig. 1 shows the basic configuration of the high-frequency link inverter. The devices S_A-S_D form an inverter circuit that feeds the transformer with a high-frequency ac voltage providing isolation between the dc source and the load.

The devices S_{11}-S_{12}, S_{31}-S_{32}, S_{21}-S_{22} and S_{41}-S_{42} are bidirectional switches and form an ac/ac converter. When the energy flows from the dc source, the ac/ac converter operates as a positive or negative rectifier. The output filter eliminates the high frequency harmonics and delivers a sinusoidal voltage to the load. The load has been modeled as a resistor, but the results can be easily extended to others applications.

Table I outlines the 4 different dc/ac converter switching states and their associated output voltage presented at primary of the transformer, V_{ab}.

Table II shows the 4 different ac/ac converter switching states and their associated output voltage presented at input of low-pass filter, V_{ef}.

TABLE I. DC/AC SWITCHING CONVERTER STATES.

S_A	S_B	S_C	S_D	V_{ab}
ON	OFF	OFF	ON	V_i
ON	ON	OFF	OFF	0
OFF	OFF	ON	ON	0
OF	ON	ON	OFF	$-V_i$

TABLE II. AC/AC SWITCHING CONVERTER STATES.

S_1	S_2	S_3	S_4	V_{ef}
ON	OFF	OFF	ON	V_{ab}
ON	ON	OFF	OFF	0
OFF	OFF	ON	ON	0
OF	ON	ON	OFF	$-V_{ab}$

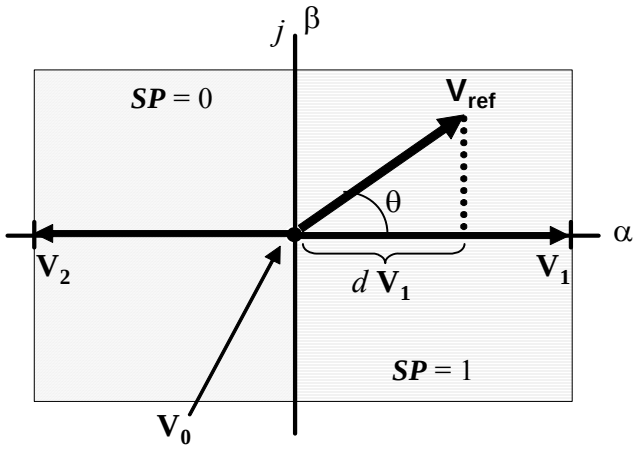

Fig. 2 State vector diagram of the dc/ac converter: $\mathbf{V_{ref}}$*, output reference voltage; d, duty ratio; sp, output voltage sign.*

B. Modulation strategy

Different modulations strategies can be derived. In order to show the converter operation, a state vector modulation is chosen. State vector modulation is easily implemented in DSP devices.

Fig. 2 describes how the state vectors are defined in this system. The relative position of the reference vector in the right or left half-plane define if the $\mathbf{V_1}$, $\mathbf{V_0}$ or the $\mathbf{V_2}$ state vectors are used, see how there are three different state vector for the converter.

The state vectors are defined as:

$$\begin{aligned} \mathbf{V_1} &= tr\,V_i + j0 \\ \mathbf{V_2} &= -tr\,V_i + j0 \\ \mathbf{V_0} &= 0 + j0 \end{aligned} \tag{1}$$

where

tr is the turn ratio of the HF transformer.

The projection of the output reference vector defines the duty-ratio *d* of the state vector. The zero vector is applied the rest of the period.

The amplitude (*m*) of the output voltage is

$$m = \sqrt{2}\ Vo_{rms} < tr\,V_i \text{ and with } f_o \text{ frequency}$$

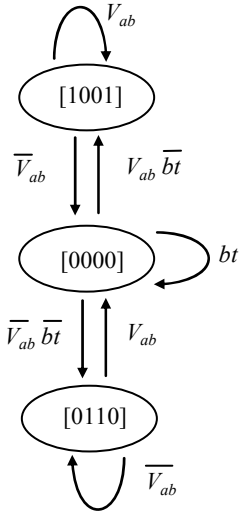

Fig. 3 Commutation strategy for the dc-ac converter if square output voltage is needed. Where bt is the blanking time, $[\mathbf{S_X}]=[S_A\ S_B\ S_C\ S_D]$ *and* V_{ab} *is the primary transformer voltage.*

The reference vector is defined by:

$$\mathbf{V_{ref}} = m\,e^{j\theta}\begin{cases} \theta = \omega t \\ \omega = 2\pi f_o \end{cases} \tag{2}$$

$$\left|\mathbf{V_{ref}}\right| = \sqrt{2}\,Vo_{rms} = m$$

Different state vector modulation strategies can be derived. The nearest two vectors are chosen to show the inverter operation. The duty ratio is defined as follows:

$$d = d_1 + d_2$$

If *Sp*=1 the nearest two vectors are $\mathbf{V_1}$ and $\mathbf{V_0}$ and

$$d_1 = \frac{m\ \cos\theta}{tr\,V_i}\ ,\ d_0 = 1 - d_1 \ \text{and}\ d_2 = 0 \tag{3}$$

If *Sp*=0 the nearest two vectors are $\mathbf{V_2}$ and $\mathbf{V_0}$ and

$$d_2 = -\frac{m\ \cos\theta}{tr\,V_i}\ ,\ d_0 = 1 - d_2 \ \text{and}\ d_1 = 0 \tag{4}$$

In (3)-(4), the duty-ratios d_1 and, d_2, define the projection of the reference vector (Fig. 2) for *SP*=1 and *SP*=0 respectively. The duty-ratio d_0 correspond to the zero vector. The HF inverter on the DC side is commanded by the duty-ratio d.

C. Commutation strategy

The commutation strategy must satisfy some rules:

a. A short circuit of the dc source is not permitted.
b. The current through the inductors cannot be interrupted.
c. A commutation strategy verifying these rules and taking advantage of the possibilities for soft switching is proposed.

The commutation strategy for the dc/ac converter is defined by the modulation strategy. If the modulation is applied to the ac-ac converter, the commutation strategy for the dc-ac converter is

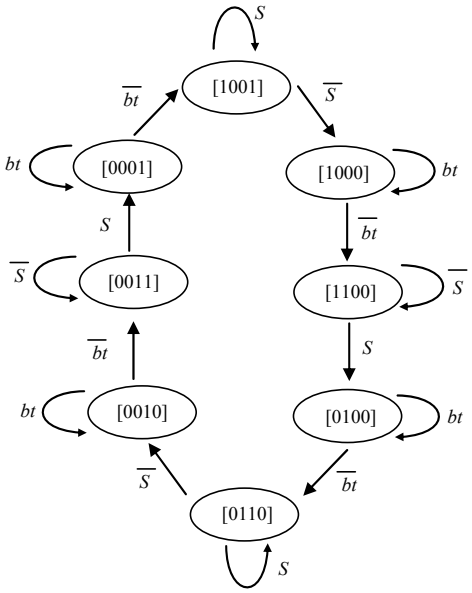

Fig. 4 Commutation strategy if PWM is applied to dc-ac converter. Where S is a switching function associated to the duty ratio, d.

defined as in Fig. 3. If the modulation is applied to the dc-ac converter, the commutation strategy is defined as in Fig. 4.

The commutation strategy for the ac/ac converter is based on a four step technique [8]. The decision about how to commute the ac/ac converter is base on the modulation strategy.

In order to generate the control signals of the ac/ac converter four input signals are required: the inductor current sign (i_L), the output voltage sign (*sp*), the transformer voltage (V_{ab}) and the pulse-width modulation signal associated to the duty-ratio *d* indicating the instantaneous value of the output voltage (*S*). The variable *S* is the switching function.

Fig. 5 shows one example of transition between S_1 ON to S_1 OFF.

A PLD implements the commutation sequence of the inverter and the ac/ac converter modulation and control scheme is implemented in a DSP.

Voltage spikes caused by the transformer secondary leakage inductance are clamped and recovered to the dc source by an energy feedback circuit presented in [4].

III. LARGE-SIGNAL AND SMALL-SIGNAL MODELS

Fig. 6 shows the switching model of the converter. The assumptions for the analysis are:

d. Ideal semiconductors.
e. Ideal HF transformer.
f. Ideal dc input source.
g. The losses in the system are neglected.
h. A resistive load is considered.
i. The switching frequency is significantly greater than the output fundamental frequency and the system cut-off frequencies.

The commutation function $S_x(t)$ is used to define the switching state of each converter switch:

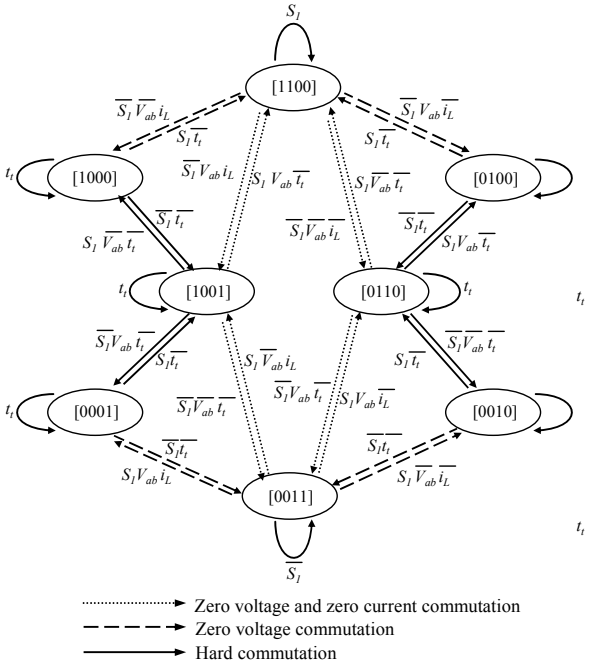

Fig. 5 Commutation between S_1 ON , S_3 OFF and S_1 OFF and S_3 ON.

$$S_x(t)=\begin{cases}0, \text{ switch open}\\ 1, \text{ switch closed}\end{cases} \tag{5}$$

In order to avoid the short-circuit of the input capacitive filter and the open circuit of the primary (in Fig. 6), it is necessary to verify that:

$$S_A+S_C=1, \qquad S_B+S_D=1 \tag{6}$$

Additionally to avoid a short circuit in the secondary of the transformer and to avoid opening the output filter inductor, the following restrictions must be fulfilled:

$$S_{11}+S_{31}=1,\ S_{21}+S_{41}=1,\ S_{12}+S_{32}=1,\ S_{22}+S_{42}=1,$$
$$(S_{11}\cdot S_{12})+(S_{31}\cdot S_{32})=1 \text{ and } (S_{21}\cdot S_{22})+(S_{41}\cdot S_{42})=1 \tag{7}$$

If the particular case where V_{ab} is a pure square signal, the expression of the input voltage of the *LC* filter using switching functions (see Fig. 3) is:

$$V_{\text{ef}}=\left(S_{ap}-S_{bp}\right)\left(S_{ec}-S_{fc}\right)trV_i \tag{8}$$

where *tr* is already defined as the turns ratio of the high-frequency isolation transformer.

Analyzing the circuit, the state equations are obtained.

$$L\frac{d}{dt}i_L=-V_o+V_{ef} \tag{9}$$

$$C\frac{d}{dt}V_o=i_L-\frac{V_o}{R} \tag{10}$$

The state-space model of the system is expressed in (11)-(15). It represents the discrete time-variant large-signal model of the dc/ac converter.

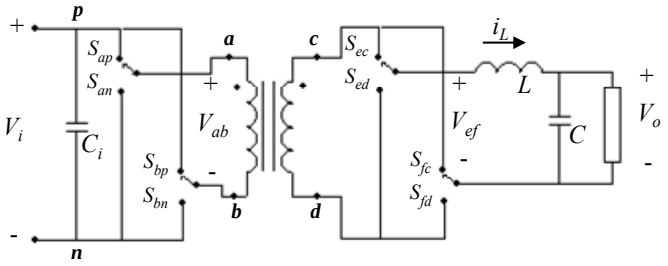

Fig. 6 Equivalent switching model of the converter.

$$\frac{d}{dt}[\mathbf{x}] = \mathbf{A}[\mathbf{x}] + \mathbf{B}[\mathbf{u}] \tag{11}$$

$$\text{where: } [\mathbf{x}] = [i_L \;\; V_o]^T \tag{12}$$

$$[\mathbf{A}] = \begin{bmatrix} 0 & -\frac{1}{L} \\ \frac{1}{C} & -\frac{1}{RC} \end{bmatrix} \tag{13}$$

$$[\mathbf{B}] = \begin{bmatrix} \frac{trV_i}{L} \\ 0 \end{bmatrix} \tag{14}$$

$$[\mathbf{u}] = \left[\left(S_{ap} - S_{bp}\right)\left(S_{ec} - S_{fc}\right) \right] \tag{15}$$

The use of the moving average technique avoids the high-frequency analysis and focuses in the low frequency components of (11). The filtering effect of inductor L and capacitor C justify the approach.

If the switching period is T_s, then the moving average of any variable x, called $\hat{x}$ is defined as:

$$\hat{x}(t) = \frac{1}{T_s} \int_{t-T_s}^{t} x(\tau) d\tau \tag{16}$$

The duty cycle is defined as in (17):

$$d = \hat{S} = \frac{1}{Ts} \int_{t-Ts}^{t} \left(S_{ap} - S_{bp}\right)\left(S_{ec} - S_{fc}\right) d\tau \tag{17}$$

The averaged state-space equation in Direct-Quadrature (DQ) coordinates is obtained using the average method and applying the DQ transformation [7], resulting in (18), where $\omega = 2\pi f$ and f is the output voltage frequency. The averaged time-invariant large-signal model is in (18). For notation simplicity, from now on, all the time-domain variables are assumed to be averaged.

$$\frac{d}{dt}\begin{bmatrix} \hat{i}_{Ld} \\ \hat{i}_{Lq} \\ \hat{v}_{Od} \\ \hat{v}_{Oq} \end{bmatrix} = \begin{bmatrix} 0 & -\omega & -\frac{1}{L} & 0 \\ \omega & 0 & 0 & -\frac{1}{L} \\ \frac{1}{C} & 0 & -\frac{1}{RC} & -\omega \\ 0 & \frac{1}{C} & \omega & -\frac{1}{RC} \end{bmatrix} \begin{bmatrix} \hat{i}_{Ld} \\ \hat{i}_{Lq} \\ \hat{v}_{Od} \\ \hat{v}_{Oq} \end{bmatrix} + \begin{bmatrix} \frac{tr\hat{V}i}{L} & 0 \\ 0 & \frac{tr\hat{V}i}{L} \\ 0 & 0 \\ 0 & 0 \end{bmatrix} \begin{bmatrix} d_d \\ d_q \end{bmatrix} \tag{18}$$

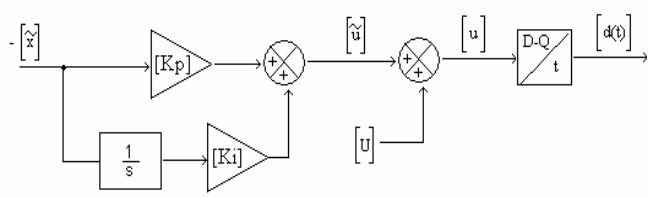

Fig. 7 Control scheme for the converter.

From (18), the steady-state values can be obtained forcing all time-derivatives to zero.

$$D_d = \frac{tr}{V_i}\left[\frac{\omega L}{R} V_{oq} + V_{od}\left(1 - \omega^2 LC\right)\right] \tag{19}$$

$$D_q = \frac{tr}{V_i}\left[-\frac{\omega L}{R} V_{od} + V_{oq}\left(1 - \omega^2 LC\right)\right] \tag{20}$$

$$I_{Ld} = \omega C V_{oq} + \frac{V_{od}}{R} \tag{21}$$

$$I_{Lq} = -\omega C V_{od} + \frac{V_{oq}}{R} \tag{22}$$

Applying the small-signal analysis to (18), the averaged time-invariant small-signal model is shown in (23).

$$\frac{d}{dt}\begin{bmatrix} \tilde{i}_{Ld} \\ \tilde{i}_{Lq} \\ \tilde{v}_{od} \\ \tilde{v}_{oq} \end{bmatrix} = \begin{bmatrix} 0 & -\omega & -\frac{1}{L} & 0 \\ \omega & 0 & 0 & -\frac{1}{L} \\ \frac{1}{C} & 0 & -\frac{1}{RC} & -\omega \\ 0 & \frac{1}{C} & \omega & -\frac{1}{RC} \end{bmatrix} \begin{bmatrix} \tilde{i}_{Ld} \\ \tilde{i}_{Lq} \\ \tilde{v}_{od} \\ \tilde{v}_{oq} \end{bmatrix} + \begin{bmatrix} \frac{trV_i}{L} & 0 \\ 0 & \frac{trV_i}{L} \\ 0 & 0 \\ 0 & 0 \end{bmatrix} \begin{bmatrix} \tilde{d}_d \\ \tilde{d}_q \end{bmatrix} \tag{23}$$

IV. CONTROL SCHEME

For closed-loop control, a linear quadratic regulator [LQR+I] in the DQ domain is proposed [6],[7].

LQR+I is used for closed-loop control since it allows obtaining an optimum multivariable controller and since all the state variables that are used for feedback can be easily sensed. The scheme is shown in Fig. 6.

The cost function for the design of the LQR regulator defines a trade-off between the output voltage error, the integral of the output voltage error and the control variables effort in order to avoid saturation. Indeed, three variables have been taken into account in the multivariable cost function.

V. SIMULATION AND EXPERIMENTAL RESULTS

A Simulation was done with the following specifications: output voltage V_o = 110 Vrms, input voltage V_i = 24 Vdc, output power P_{omax} = 160 W, output voltage frequency f = 50 Hz, f_s=20kHz, L=2mH and C=10uF.

The large-signal model in (14) allows simulating the converter. The operation output voltage and inductor current in closed-loop are shown in Figs. 8, 9.

An experimental prototype has been implemented using functional modules. It is shown in Fig. 10. Experiments have been performed in order to verify the characteristics of the proposed circuit.

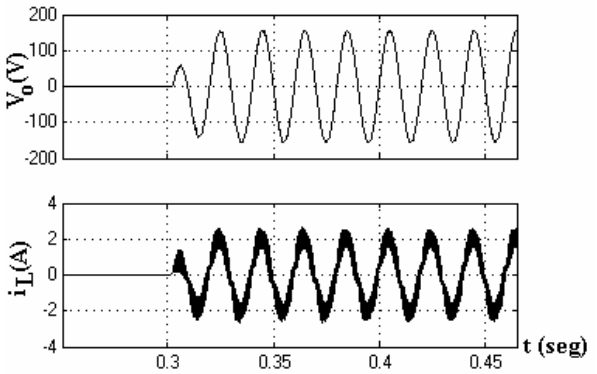

Fig. 8 *Closed-loop simulation waveform:* V_o *and* i_L. *Start-up of the converter.*

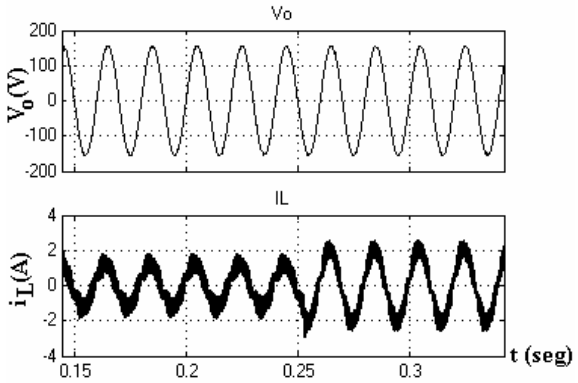

Fig. 9 Closed-loop simulation waveforms: V_o *and* i_L. *Power step from 50% to 100% of rated power.*

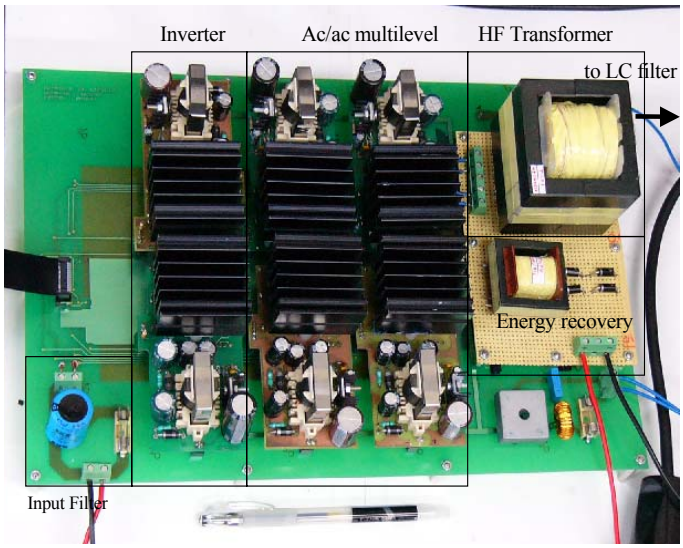

Fig. 10 DC/AC Converter prototype.

The experimental conditions are: V_i=24Vdc, V_o=110Vrms, P_{omax}=160 W, f=50Hz, f_s=20kHz, tr= 8.33, L=2mH and C=10uF.

Fig. 11 includes the output voltage and inductor current during the start-up of the converter. The results show that the response is very fast.

Figs. 12 and 13 show the evolution of the output voltage and the inductor current during a load transient. The response is very fast and there is no overshoot.

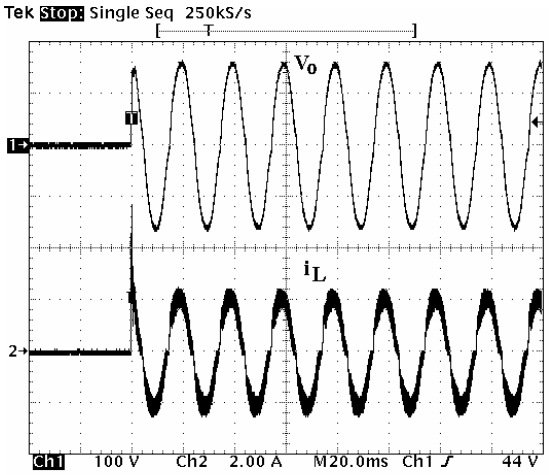

Fig. 11 Experimental results: V_o *and* i_L *in closed-loop. Start-up of the converter.*

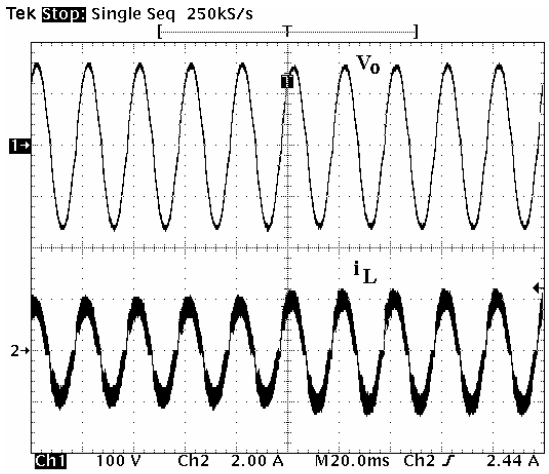

Fig. 12 Experimental results: V_o *and* i_L *in closed-loop. Power step from 85% to 100% of rated power.*

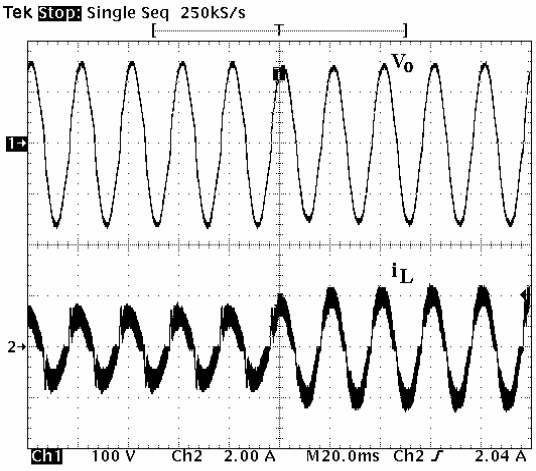

Fig. 13 Experimental results: V_o *and* i_L *in closed-loop. Power step from 50% to 100% of rated power.*

VI. CONCLUSIONS

This paper presents a comprehensive study of a dc/ac inverter with high-frequency isolation and bidirectional power flow capability. The benefits of this topology are: reduced number of conversion stages, no dc-link required, and bi-directional operation capability. The LQR+I control approach for a dc/ac topology with high-frequency isolation is presented. The LQR+I is an effective way to implement a multivariable control. Simulations of the proposed control method have proven its good performance in terms of response time and overshoot. The experimental results correlate perfectly with the model and its performance with small overshoot and very low steady-state error. These results show the benefits of the LQR+I control technique.

REFERENCES

[1]. Harada, K.; Sakamoto, H.; Shoyama, M., "Phase-controlled DC-AC converter with high-frequency switching", IEEE Trans. Power Electronics, Vol.: 3, Oct. 1988, pp. 406 –411.

[2]. Aoki, T.; Yotsumoto, K.; Muroyama, S.; Kenmochi, Y., "A new uninterruptible power supply with a bidirectional cycloconverter", Intl. Telecom. Energy Conf., 1990. INTELEC '90, pp. 424 –429.

[3]. Fujimoto, H.; Kuroki, K.; Kagotani, T.; Kidoguchi, H., "Photovoltaic inverter with a novel cycloconverter for interconnection to a utility line", IEEE IAS Annual Meeting, IAS '95., pp. 2461 -2467.

[4]. Sree, H.; Mohan, N., "Voltage sag mitigation using a high-frequency-link cycloconverter-based DVR," IEEE Industrial Electronics Soc. Conf., 2000. IECON'00, pp. 344 –349.

[5]. Lima, F.; Anunciada, V. "Novel active uninterruptible power supply using high frequency ZVS cycloconverters," IEEE Intl. Symp. Industrial Electronics, 2000. ISIE'00, pp. 112 -117.

[6]. Alepuz, S.; Salaet, J.; Gilabert, A. and Bordonau J. "Control of three-level VSIs with a LQR-based gain-scheduling technique applied to DC-link neutral voltage and power regulation", IECON2002, pp. 914-912.

[7]. Salaet, J.; Alepuz, S.; Gilabert, A.; Bordonau, J.; Peracaula, J**.** "D-Q modeling and control of a single-phase three-level boost rectifier with power factor correction and neutral-point voltage balancing", PESC2002, pp.514-519.

[8]. Beristáin J. A. "Inversores bidireccionales con aislamiento en alta frecuencia para aplicaciones de energías renovables", PhD. Dissertation, Technical University of Catalonia, June 2005.

Beristáin J. José A. was born in Córdoba, Mexico on August 15, 1973. He received the Master´s degree in Electronic Engineering from National Center for Technological Development and Research (cenidet) Cuernavaca México , in 1998 and Ph. D. degree in Electronic Engineering from Technical University of Catalonia (UPC), Barcelona Spain, in 2005.

He is currently a Professor of Electrical and Electronics Engineering at Technologic Institute of Sonora, Cd. Obregón, Sonora, México. His teaching and research interest are in application of power electronics in renewable energy systems.

Bordonau F. Josep was born in Sitges, Spain. He received the M.Sc. and Ph. D. degrees in electrical engineering (with honors) form Technical University of Catalonia, Barcelona, Spain, in 1984 and 1990, respectively.

He has been Lecture and Assistant Professor in the Electronics Engineering Department, Technical University of Catalonia, where he has been an Associate Professor since 1991. He has been active in research projects with international companies and institutions, and was principal researcher of more than 25 research projects. He has authored more than 50 journal and conference papers and is the holder of a European patent. His fields of interest are ac power converters applied to renewable energy systems and energy management systems.

Busquets M. Sergio was born in Barcelona, Spain, on February 14, 1974. He graduated in electrical engineering from the Technical University of Catalonia, Spain, in 1999, received the M.S. degree in electrical engineering from the Virginia Polytechnic Institute and State University, Blacksburg, VA, in 2001, and the Ph.D. degree in electrical engineering from the Technical University of Catalonia in 2006. From 2001 to 2002 he was with Crown International, Inc. He is currently an Assistant Professor in the Electronics Engineering Department of the Technical University of Catalonia. His research interests include multilevel conversion, power converter modeling, control and automated design, power factor correction, and EMI suppression techniques.

Rocabert S. Joan was born in Barcelona, Spain. He graduated in electrical engineering from the Technical University of Catalonia, Spain, in 2002. His research interests include multilevel conversion, power converter modeling, control and automated design, power factor correction, and EMI suppression techniques.

Murillo V. Ismael was born in Pueblo Yaqui, Mexico on June 16, 1961. He received the Master´s degree in Mechanic Engineering from National Autonomous University of México (UNAM), in 2004.

He is currently a Professor of Electrical and Electronics Engineering at Technologic Institute of Sonora, Cd. Obregón, Sonora, México. His teaching and research interest are in application of Electric Machinery in Utilization of energy.